

# Decorrelation of anisotropic flows along the longitudinal direction

Long-Gang Pang<sup>1</sup>, Hannah Petersen<sup>1,2,3</sup>, Guang-You Qin<sup>4</sup>, Victor Roy<sup>2</sup> and Xin-Nian Wang<sup>4,5</sup>,

<sup>1</sup>*Frankfurt Institute for Advanced Studies, Ruth-Moufang-Strasse 1, 60438 Frankfurt am Main, Germany*

<sup>2</sup>*Institute for Theoretical Physics, Goethe University,*

*Max-von-Laue-Strasse 1, 60438 Frankfurt am Main, Germany*

<sup>3</sup>*GSI Helmholtzzentrum für Schwerionenforschung, Planckstr. 1, 64291 Darmstadt, Germany*

<sup>4</sup>*Key Laboratory of Quark & Lepton Physics (MOE) and Institute of Particle Physics,  
Central China Normal University, Wuhan 430079, China and*

<sup>5</sup>*Nuclear Science Division MS70R0319, Lawrence Berkeley National Laboratory, Berkeley, CA 94720*

The initial energy density distribution and fluctuation in the transverse direction lead to anisotropic flows of final hadrons through collective expansion in high-energy heavy-ion collisions. Fluctuations along the longitudinal direction, on the other hand, can result in decorrelation of anisotropic flows in different regions of pseudo rapidity ( $\eta$ ). Decorrelation of the 2nd and 3rd order anisotropic flows with different  $\eta$  gaps for final charged hadrons in high-energy heavy-ion collisions is studied in an event-by-event (3+1)D ideal hydrodynamic model with fully fluctuating initial conditions from A Multi-Phase Transport (AMPT) model. The decorrelation of anisotropic flows of final hadrons with large  $\eta$  gaps are found to originate from the spatial decorrelation along the longitudinal direction in the AMPT initial conditions through hydrodynamic evolution. The decorrelation is found to consist of both a linear twist and random fluctuation of the event-plane angles. The agreement between our results and recent CMS data in most centralities suggests that the string-like mechanism of initial parton production in AMPT model captures the initial longitudinal fluctuation that is responsible for the measured decorrelation of anisotropic flows in Pb+Pb collisions at LHC. Our predictions for Au+Au collisions at the highest RHIC energy show stronger longitudinal decorrelation, indicating larger longitudinal fluctuations at lower beam energies. Our study also calls into question some of the current experimental methods for measuring anisotropic flows and extraction of transport coefficients through comparisons to hydrodynamic simulations that do not include longitudinal fluctuations.

PACS numbers: 12.38.Mh, 25.75.Ld, 25.75.Gz

## I. INTRODUCTION

Anisotropic flows or Fourier coefficients  $\bar{V}_n = v_n \exp(in\Psi_n)$  of the distribution of final charged hadrons in azimuthal angle are important observables in high-energy heavy-ion collisions. They provide critical information about the initial state and evolution of the strongly coupled Quark Gluon Plasma (QGP). They have been used to extract the ratio of shear viscosity over entropy density  $\eta_v/s$  of the QGP through comparisons between event-by-event viscous hydrodynamic calculations and experimental measurements at the Relativistic Heavy-ion Collider (RHIC) and the Large Hadron Collider (LHC) [1–10]. However, it is well known that  $v_n$ 's from hydrodynamic simulations are very sensitive to initial state fluctuations [11, 12]. For example, values of  $\eta_v/s$  extracted from fitting experimental data on  $v_2$  with viscous hydrodynamic simulations differ between the Monte Carlo Glauber (MC-Glauber) and Monte Carlo Color Glass Condensate (MC-CGC) models for initial state conditions, while all other parameters in the viscous hydrodynamic model are kept fixed [13–15]. In addition, many models of initial conditions for viscous hydrodynamic simulations fail to describe the second ( $v_2$ ) and the third ( $v_3$ ) order harmonic flow coefficients simultaneously in ultra central collisions [16]. The transverse momentum and pseudo rapidity dependent event plane angles  $\Psi_n(p_T, \eta)$  in 3+1D hydrodynamic simulations in-

cluding full fluctuations in both transverse and longitudinal directions have not been fully investigated yet.

The initial energy density distribution and fluctuations of the QGP in the transverse plane have been studied in detail in event-by-event hydrodynamics with initial conditions given by MC-Glauber, MC-CGC [11, 17], UrQMD [18], EPOS [19], AMPT [20] and IP-Glasma [21]. Fluctuations in the transverse plane not only give rise to odd flow harmonics but also significant even and odd  $v_n$  in ultra central collisions [22]. They also result in  $p_T$  dependent event planes, which break down the flow factorization  $v_{n,n}(p_{T1}, p_{T2}) = v_n(p_{T1})v_n(p_{T2})$  [23–27], where  $v_{n,n}$  is obtained from the long-range two-particle correlation function. The decorrelation between event planes for particles with fixed transverse momentum  $p_{T1}$  and the event plane determined by particles in the full  $p_T$  range may even give rise to negative  $v_n$  at  $p_{T1}$  for ultra central collisions.

Studies of fluctuations along the longitudinal direction and their effects on anisotropic flows of final charged hadrons have only recently been started. Energy density fluctuations in spatial rapidity were first studied in a Boltzmann parton and hadron transport + hydrodynamic hybrid approach [28]. Later it was observed that the elliptic flow  $v_2$  is noticeably suppressed in the presence of longitudinal fluctuations in event-by-event (3+1)D ideal hydrodynamics with AMPT initial conditions [20]. This was later confirmed by another inde-

pendent study within the AMPT model [29] in which the pseudo rapidity window for event plane determination has been varied. A comparison between results from (3+1)D ideal hydrodynamics and direct AMPT model simulations shows that both models convert the fluctuation in the initial energy momentum tensor in coordinate space to a decorrelation of anisotropic flows for final charged hadrons in momentum space [30]. These early studies indicate that the longitudinal structure of the initial states of QGP and their evolution play an important role in extracting the transport coefficients from experimental data and may shed light on the  $v_n$  puzzle in ultra central collisions.

Variations of event plane angles  $\Psi_n(\eta)$  in the longitudinal direction can consist of a linear twist and random fluctuations along the  $\eta$  direction. The linear twist is a continuous rotation of event plane angles from project to target beam direction in heavy-ion collisions. The twist in gluon number density distributions was first suggested in the CGC model [31, 32], considering the trapezoidal distribution of gluon number density  $\rho_g(\eta, x_\perp)$  associated with asymmetric forward and backward participants in projectile and target nuclei in non-central heavy-ion collisions. The twist of event plane angles was also suggested by Bozek [33] in a wounded-nucleon model, where fireballs in relativistic heavy-ion collisions may be torqued with the assumption that the forward (backward) wounded nucleons emit particles preferably in the forward (backward) direction. The twist in the energy density distribution along the longitudinal direction in the initial state will lead to a torqued collective flow and torqued momentum distributions in different rapidity windows. On top of the twist, there is also a random fluctuation of event plane angles  $\Psi_n(\eta)$  due to the finite number of particles in a given window of pseudo-rapidity. Both the twist and random fluctuations in the initial energy density distribution lead to variations of event plane angles  $\Psi_n(\eta)$  along the longitudinal direction and decorrelation of anisotropic flows of final hadrons with large pseudo-rapidity gaps. It is important to separate effects of these two mechanisms for decorrelation of anisotropic flows along the longitudinal direction.

Many techniques have been proposed to study the longitudinal structure of final hadron production in heavy-ion collisions and the underlying mechanisms. For example, three particle correlations were suggested to measure the twist effect [34] in heavy-ion collisions at RHIC. One can also characterize the longitudinal fluctuation in terms of coefficients in the Legendre polynomial expansion of two-particle correlations in pseudo-rapidity [35–37]. The most intuitive method is to measure the forward-backward event plane angles [29, 33, 38] or anisotropic flow differences [30] with varying pseudo rapidity gaps  $\Delta\eta$ . These methods are used within the torqued fireball model [33], (3+1)D hydrodynamics model [30, 33] and the AMPT model [29, 30, 39] to study the decorrelation of event plane angles or anisotropic flows along the pseudo rapidity direction. Jia et al. [38, 39] also proposed

an “event-shape twist” technique to study the event plane decorrelation due to the twist in initial energy density distributions by selecting events with big forward-backward (FB) event plane angle differences. By selecting events with vanishingly small FB event plane angle differences, one can then eliminate the twist effect and the measured decorrelation of anisotropic flows with finite pseudo rapidity gaps should be caused only by random fluctuations of event plane angles [30].

The most recent CMS measurements [40] use a different definition of correlations of anisotropic flows which intends to remove contributions from short range correlations that can arise from the longitudinal expansion of hot spots along  $\eta$ , non-flow correlations from jet fragments, Bose-Einstein correlation and resonance decays. In this paper, we carry out a study of such correlations within an event-by-event (3+1)D ideal hydrodynamic model with AMPT initial conditions and compare with CMS experimental data. We will investigate the decorrelation of 2nd and 3rd order anisotropic flows along the pseudo-rapidity direction. The rest of this article is organized as follows. In Sec. II we introduce the definition of the longitudinal decorrelation, the (3+1)D ideal hydrodynamic model and the fluctuating initial conditions employed in our study. Results for Pb+Pb collisions at LHC are compared with CMS experimental data and predictions for Au+Au collisions at RHIC are presented in Sec. III. In Sec. IV we investigate fluctuations and the decorrelation in the initial state in coordinate space. The twist of event plane angles and random fluctuations are studied in Sec. V for all centralities to illustrate the non-linear decorrelation in most central collisions. A summary and discussions on effects of longitudinal fluctuations on anisotropic flow and di-hadron correlations are given in Sec. VI.

## II. METHOD AND MODEL

### A. Decorrelation of anisotropic flow in pseudo rapidity

We start with the definition of the correlation observable [40] proposed by CMS. The pseudo-rapidity coverages of  $\eta^a \in (-2.4, 2.4)$  for Pb+Pb collisions at  $\sqrt{s_{NN}} = 2.76$  TeV and  $\eta^a \in (-1.5, 1.5)$  for Au+Au collisions at  $\sqrt{s_{NN}} = 200$  GeV are divided into 16 and 10 rapidity bins, respectively, with equal bin size  $\Delta\eta = 0.3$ . Particles from reference pseudo-rapidity windows  $\eta_b \in (3.0, 5.0)$  and  $\eta_b \in (2.5, 4.0)$  are used in Pb+Pb and Au+Au collisions, respectively, to be correlated with particles at  $\eta^a$  which is denoted as  $V_{n\Delta}(\eta^a, \eta^b)$  to remove short range correlations in the denominator. The ratio between  $V_{n\Delta}(-\eta^a, \eta^b)$  and  $V_{n\Delta}(\eta^a, \eta^b)$  (for  $\eta_a > 0$ ) serves as a measure of the decorrelation of anisotropic flows as a function of pseudo rapidity gap  $\Delta\eta = 2\eta^a$ ,

$$r_n(\eta_a, \eta_b) = V_{n\Delta}(-\eta_a, \eta_b)/V_{n\Delta}(\eta_a, \eta_b)$$

$$= \frac{\langle v_n(-\eta_a)v_n(\eta_b) \cos[n(\Psi_n(-\eta_a) - \Psi_n(\eta_b))] \rangle}{\langle v_n(\eta_a)v_n(\eta_b) \cos[n(\Psi_n(\eta_a) - \Psi_n(\eta_b))] \rangle}, \quad (1)$$

which is also called  $\eta$ -dependent factorization ratio. The di-hadron correlation function factorizes along  $\eta$  and  $r_n(\eta_a, \eta_b) = 1$  if there are no longitudinal fluctuations. Otherwise, the correlation between  $\eta_a$  and  $\eta_b$  is stronger than that between  $-\eta_a$  and  $\eta_b$ , and the factorization in  $\eta$  breaks down ( $r_n(\eta_a, \eta_b) < 1$ ).

A global twist of event planes or decreasing long range correlation with increasing pseudo rapidity gap  $\Delta\eta$  can lead to this kind of breaking of factorization. Events with pure random fluctuations of  $v_n(\eta)$  and  $\Psi_n(\eta)$  do not contribute either to numerator or the denominator of  $r_n(\eta_a, \eta_b)$ .

In practice we use the  $\vec{Q}_n$  vector to quantify the  $n$ th order anisotropic flow in a given pseudo-rapidity bin which is defined as,

$$\begin{aligned} \vec{Q}_n &\equiv Q_n e^{in\Phi_n} = \frac{1}{N} \sum_{j=1}^N e^{in\phi_j} \\ &= \frac{\int \exp(in\phi) \frac{dN}{d\eta dp_T d\phi} dp_T d\phi}{\int \frac{dN}{d\eta dp_T d\phi} dp_T d\phi}, \end{aligned} \quad (2)$$

where  $\phi_j = \arctan(p_{yj}/p_{xj})$  is the azimuthal angle of the  $j$ th particle as determined by its transverse momentum. In hydrodynamic simulations, smooth particle spectra  $dN/d\eta dp_T dp_T d\phi$  and phase space integration over  $p_T$  and azimuthal angle  $\phi$  are used to calculate the  $\vec{Q}_n$  vector. In this case, the  $\vec{Q}_n$  vector will be identical to the flow vector  $\vec{v}_n$  and the decorrelation of anisotropic flows in 2 different rapidity bins  $-\eta_a$  and  $\eta_a$  becomes,

$$r_n(\eta_a, \eta_b) = \frac{\langle \vec{Q}_n(-\eta_a) \vec{Q}_n^*(\eta_b) \rangle}{\langle \vec{Q}_n(\eta_a) \vec{Q}_n^*(\eta_b) \rangle} \quad (3)$$

For collisions at both RHIC and LHC energies we follow the CMS analysis and use the transverse momentum cut  $[0.3, 3.0)$  GeV/c for particles in pseudo-rapidity windows  $\eta_a$  and  $[0, \infty)$  for particles in  $\eta_b$ .

## B. Event-by-event (3+1)D hydrodynamics

A (3+1)D ideal hydrodynamical model [20, 41] is employed to study the decorrelation of anisotropic flows in different rapidity windows in Pb+Pb collisions at  $\sqrt{s_{NN}} = 2.76$  TeV and Au+Au collisions at  $\sqrt{s_{NN}} = 200$  GeV with fluctuating initial conditions from AMPT [42]. The initial state local energy momentum tensor is constructed from the coordinates  $(t_i, x_i, y_i, z_i)$  and four-momenta  $(m_{Ti} \cosh Y_i, p_{xi}, p_{yi}, m_{Ti} \sinh Y_i)$  of partons when they cross the  $\tau_0 = \sqrt{t^2 - z^2}$  hyperbolic line. The initial energy momentum tensor is constructed in

$(\tau, x, y, \eta_s)$  coordinates according to

$$\begin{aligned} T^{\mu\nu}(\tau_0, x, y, \eta_s) &= K \sum_i \frac{p_i^\mu p_i^\nu}{p_i^0} \frac{1}{\tau_0 \sqrt{2\pi\sigma_{\eta_s}^2}} \frac{1}{2\pi\sigma_r^2} \\ &\times \exp \left[ -\frac{(x-x_i)^2 + (y-y_i)^2}{2\sigma_r^2} - \frac{(\eta_s - \eta_{si})^2}{2\sigma_{\eta_s}^2} \right], \end{aligned} \quad (4)$$

where,

$$p_i^\mu = (m_{Ti} \cosh(Y_i - \eta_s), p_{xi}, p_{yi}, m_{Ti} \sinh(Y_i - \eta_s)/\tau_0)$$

are four-momenta of partons in  $(\tau, x, y, \eta_s)$  coordinates. Local thermalization is assumed in coordinate space through a normalized Gaussian distribution with widths  $\sigma_r$  in transverse coordinates  $r$  and  $\sigma_{\eta_s}$  in spatial rapidity  $\eta_s$ . The same smearing widths  $\sigma_r = 0.6$  fm and  $\sigma_{\eta_s} = 0.6$  as in previous studies [20] are used in this calculation, and different values of  $\sigma_{\eta_s} = 0.4, 0.6, 0.8$  are employed to study the sensitivity of the factorization ratio  $r_n(\Delta\eta)$  to short range correlations from smearing. The partial chemical equilibrium equation of state (EOS) s95p-PCE-v0 from lattice QCD calculations [43] is used in the hydrodynamic model. This EOS is known to produce softer transverse momentum spectra and bigger anisotropic flows than the chemical equilibrium EOS [20]. A parameter  $K$  in Eq. (4) is used to fit the final charged hadron multiplicity at mid-rapidity for most central collisions. With the s95p-PCE-v0 EOS, one finds  $K = 1.5$  for LHC energy and  $K = 1.4$  for RHIC energy. The same values are used for all other centralities. The initial thermalization time  $\tau_0$  is unchanged from previous simulations [20] where  $\tau_0 = 0.2$  fm for LHC and  $\tau_0 = 0.4$  fm for RHIC energy.

AMPT uses HIJING [44] to generate initial partons from hard and semi-hard scatterings and excited strings from soft interactions. The number of mini-jet partons per binary nucleon-nucleon collision in hard and semi-hard scatterings follow a Poisson distribution with the mean value given by the jet cross section. The number of excited strings is equal to the number of participant nucleons in each event. The AMPT model uses a string-melting mechanism to convert strings into partons that will follow a parton cascade and eventually hadronize according to a parton recombination model. We run AMPT in Cartesian coordinates to the end and extract the initial condition at a given initial invariant time  $\tau_0$  for our hydrodynamic simulations. The Monte Carlo Glauber model is used in HIJING to determine the number of binary collisions and the number of participants. Besides random fluctuations from mini-jet partons, the parton density fluctuates along longitudinal direction according to the length of strings. There are basically three types of strings,

- strings associated with each wounded nucleon (between a valence quark and a diquark),
- single strings between  $q - \bar{q}$  pairs from quark annihilation and gluon fusion processes,

- strings between one hard parton from parton scatterings and valence quark or di-quark in wounded nucleons.

Fluid expansion of the tube-like energy density from these strings results in long range correlations in  $\eta$  (ridge) in the final state. Fluctuations of string lengths together with the asymmetric distribution between forward-backward participants provide large fluctuations along the longitudinal direction. Length fluctuations of color flux tubes are also assumed by Bozek in the torqued fireball model in order to explain the breakdown of factorization along  $\eta$  in p+Pb collisions [45].

For careful comparisons with experimental data involving event-by-event fluctuations, centrality selections have to be chosen consistently with similar event classes. In the CMS experiment [40], centrality classes in Pb+Pb collisions at  $\sqrt{s_{NN}} = 2.76$  TeV/n are determined by the total energy deposited in the hadronic forward (HF) calorimeters, and the results are equivalent to those obtained by total number of final charged hadrons. In our calculations in this paper, we determine centrality classes by the number of initial partons, which is proportional to the number of final charged hadrons after hydrodynamic simulations.

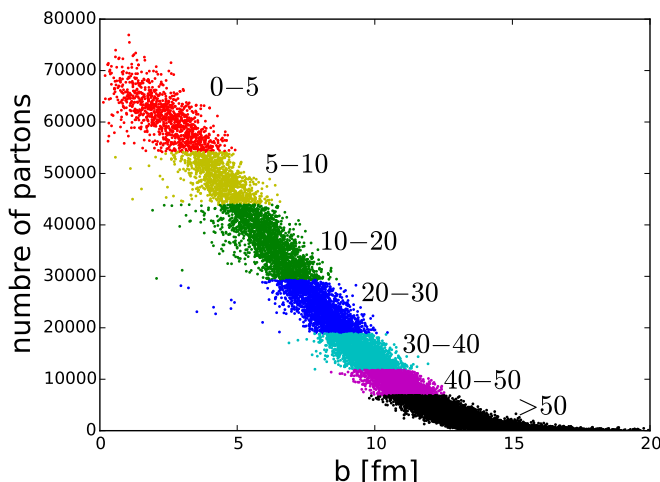


Figure 1: (Color online) The centrality classes determined by number of initial partons versus the impact parameter ranges.

We use 100,000 minimum bias AMPT events within the range  $[r_{min}, r_{max}] = [0, 20]$  fm of the impact parameter to provide initial conditions on a hyperbolic surface at an initial time  $\tau = \tau_0$ . Events are grouped into different centrality classes according to the percentage of events ordered by the total number of initial partons. For example, events in the 0-5% centrality are selected from the top 5% of events that have the highest number of initial partons, and so on. The scatter plot in Fig. 1 shows different centrality classes determined from this method and their corresponding impact parameters. Obviously, centrality classes determined by the number of initial par-

tons are quite different from those determined by ranges of impact parameters.

By selecting similar events for each centrality class as the CMS experiment at LHC, our current simulations agree with experimental data better than the previous results with centralities determined by ranges of impact parameters [30].

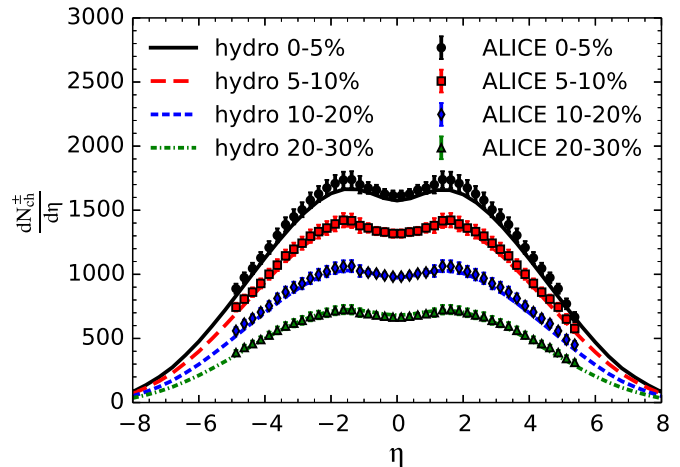


Figure 2: (Color online) Charged multiplicity distributions as a function of pseudo-rapidity for Pb+Pb  $\sqrt{s_{NN}} = 2.76$  TeV collisions from event-by-event (3+1)D hydrodynamics compared with ALICE measurements at LHC.

We fix the parameters in our event-by-event hydrodynamic model by comparing to experimental data on  $dN_{ch}/d\eta$  for the 0-5% central collisions. The charged multiplicity as a function of pseudo-rapidity  $dN_{ch}/d\eta$  in other centralities from our event-by-event hydrodynamic simulations agree with ALICE measurements [46] rather well as shown in Fig. 2.

Shown in Fig. 3 are transverse momentum spectra for  $\pi^+$  in centrality classes 0 – 5%, 5 – 10%, 10 – 20%, 20 – 30% and 30 – 40% from our event-by-event hydrodynamic calculations (solid lines) as compared with ALICE measurements (solid circles). Our calculations with (3+1)D ideal hydrodynamic model with partial chemical equilibrium EOS agree very well with the experimental data especially in the low  $p_T$  region. They, however, under-estimate the particle production at high  $p_T$ . High  $p_T$  spectra are not expected to influence  $p_T$ -integrated anisotropic flows that are used to calculate the factorization ratio  $r_n(\Delta\eta)$ .

### III. RESULTS ON FACTORIZATION RATIOS

The factorization ratios  $r_2$  and  $r_3$  as a function of  $\eta_a$  in 6 centralities from 0 – 5% to 40 – 50% collisions are shown in Figs. 4 and 5, for Pb+Pb collisions at  $\sqrt{s_{NN}} = 2.76$  TeV and Au+Au collisions at  $\sqrt{s_{NN}} = 200$  GeV from our event-by-event (3+1)D hydrodynamic simulations,

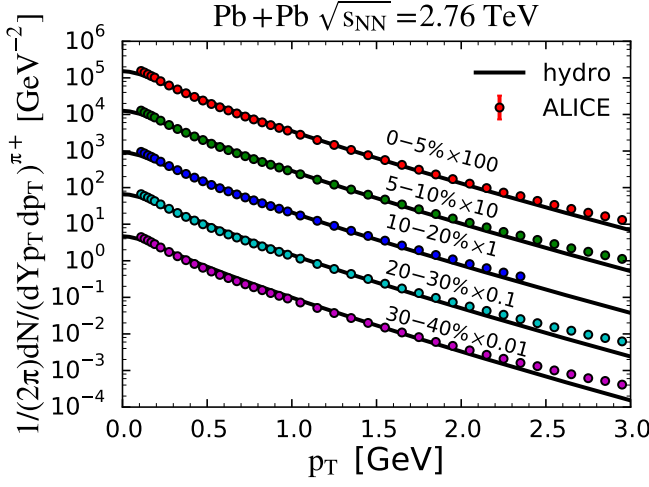


Figure 3: (Color online) Transverse momentum spectra of  $\pi^+$  in Pb+Pb collisions at  $\sqrt{s_{NN}} = 2.76$  TeV in different centralities from event-by-event (3+1)D hydrodynamics (solid lines) compared with ALICE measurements at LHC (solid circles).

and compared with CMS measurements for Pb+Pb col-

lisions at  $\sqrt{s_{NN}} = 2.76$  TeV [40]. The factorization ratio for the second anisotropic flow  $r_2(\eta_a, \eta_b)$  with the reference rapidity window  $4.4 < \eta_b < 5.0$  from event-by-event hydrodynamic simulations show a rather nice agreement with CMS measurements for all centralities except 0–5% central collisions. The splitting of the factorization ratios with 2 different reference windows  $\eta_b$  from hydrodynamic calculations is tiny. This suggests that the current definition of the factorization ratio is insensitive to short range correlations from the hydrodynamic expansion of hot spots and resonance decay. Both results fit better the CMS measurements with the reference rapidity window  $4.4 < \eta_b < 5.0$ , where short range jet-like correlations are strongly suppressed. For 0–5% central collisions, the decorrelation from event-by-event hydrodynamic simulations is more linear than CMS measurements. Hydrodynamic predictions for RHIC energy have quite similar centrality dependence, with much stronger decorrelation along pseudo-rapidity than LHC energy. This is reasonable since fluctuations at RHIC energy are much bigger than LHC energy. The prediction is consistent with anisotropic flow measurements at RHIC and LHC, where the variation of  $v_2$  in  $|\eta| < 2.5$  is much bigger for RHIC than LHC [47].

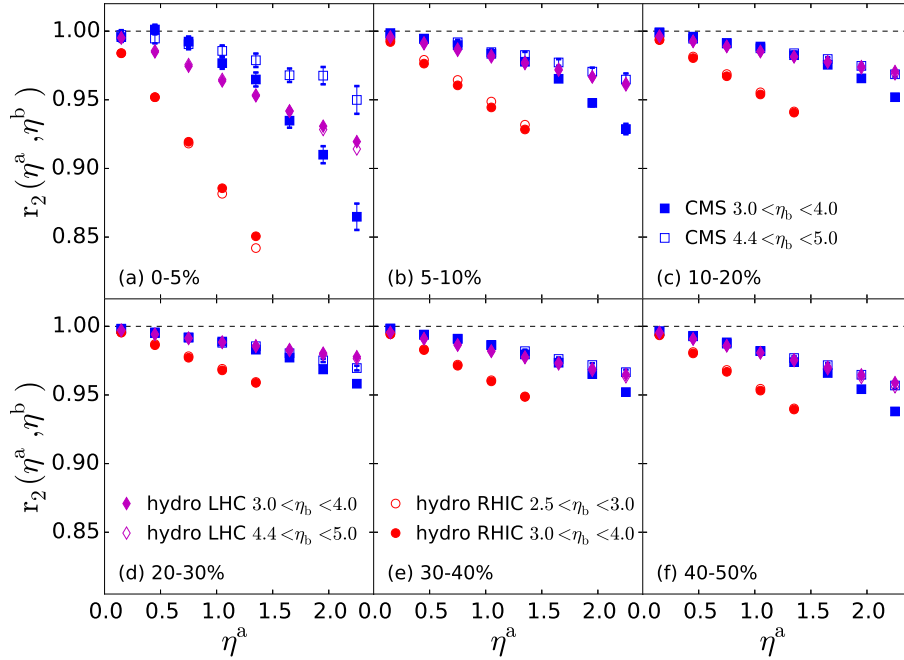


Figure 4: (Color online) The factorization ratio  $r_2$  as a function of  $\eta^a$  for  $3.0 < \eta^b < 4.0$  and  $4.4 < \eta^b < 5.0$ , in Pb+Pb collisions at  $\sqrt{s_{NN}} = 2.76$  TeV (open and solid diamonds), and for  $2.5 < \eta^b < 3.0$  and  $3.0 < \eta^b < 4.0$  in Au+Au collisions at  $\sqrt{s_{NN}} = 200$  GeV (open and solid circles) from event-by-event 3 + 1D ideal hydrodynamic simulations as compared with CMS experimental data [40] for Pb+Pb collisions at  $\sqrt{s_{NN}} = 2.76$  TeV/n (empty and solid squares) in 6 different centralities.

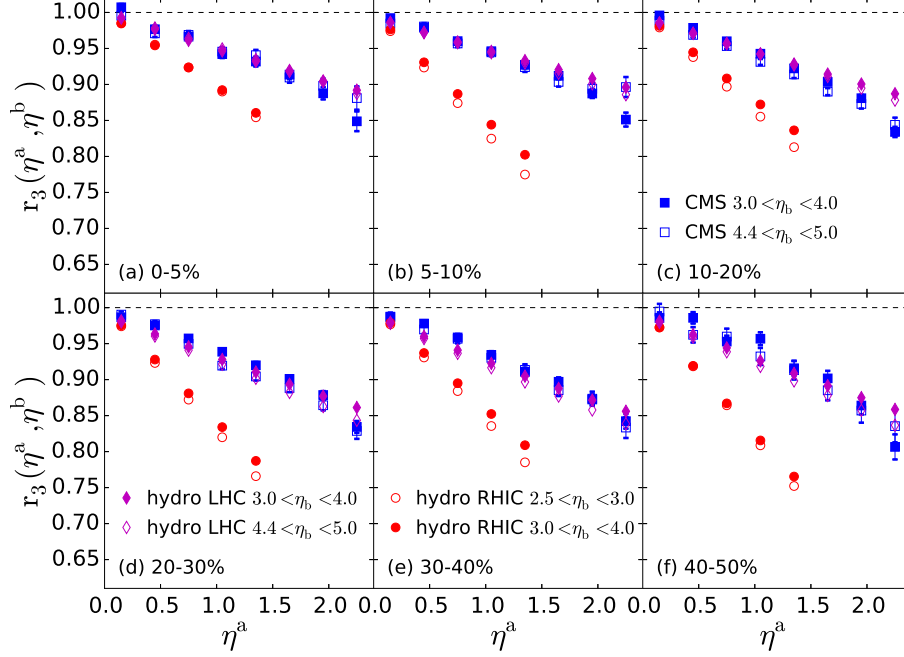


Figure 5: (Color online) The same as Fig. 4 except for factorization ratio  $r_3$ .

It is interesting that the decorrelation in the factorization ratio as a function of  $\eta^a$  at both RHIC and LHC energy have a linear behavior, which can be parameterized with,

$$r_n(\eta^a, \eta^b) \approx e^{-2F_n^\eta \eta^a}, \quad (5)$$

where the factor  $F_n^\eta$  can be considered as a measure of the factorization breakdown. The decorrelation in the longitudinal direction can be caused by a systematic twist and additional random fluctuations. The twist of event planes originates from the forward-backward asymmetry for the transverse distribution of participant projectile and target nucleons. It is not expected to have a strong dependence on the beam energy. The stronger decorrelation we observe in Figs. 4 and 5 at RHIC as compared to that at LHC is caused mainly by larger fluctuations due to smaller number of initial partons. In the AMPT model which uses HIJING for initial semi-hard jet production and soft string excitation, the smaller number of initial partons at RHIC energy relative to LHC is due to smaller number of mini-jets and shorter length of soft strings. For lower beam energies at RHIC, fluctuations of the string length in the initial state are the main mechanism for decorrelation in the longitudinal direction. This also explains the strong decorrelation observed in the most central collisions. The experimental observation of such a stronger decorrelation in pseudo-rapidity at RHIC will provide another confirmation about the string picture of initial parton production. This picture captures most

of the longitudinal fluctuations and correlations in coordinate space, which are converted into the longitudinal decorrelation and long range correlation of final charged hadrons in momentum space.

#### IV. LONGITUDINAL DECORRELATION IN THE INITIAL STATE

To investigate further the origin of the final-state decorrelation of event planes, we investigate fluctuations of the initial-state geometry in terms of spatial eccentricity vectors at different space-time rapidity  $\eta_s$ ,

$$\vec{\epsilon}_n(\eta_s) = \epsilon_n \exp(i\Psi_n) = \frac{\int d\mathbf{r}_\perp^2 \epsilon(r, \phi, \eta_s) e^{in\phi} r^n}{\int d\mathbf{r}_\perp^2 \epsilon(r, \phi, \eta_s) r^n}. \quad (6)$$

In order to get a better linear correspondence between initial state eccentricity  $\epsilon_n(\eta_s)$  and final-state momentum anisotropy  $v_n(\eta)$ , the distribution of local energy density  $\epsilon(r, \phi, \eta_s)$  in each spatial rapidity window is re-centered according to the center of mass in this rapidity window. However, we should keep in mind that two adjacent fluid cells in rapidity direction do interact with each other in (3+1)D hydrodynamics, which introduces non-linear correlation between  $\epsilon_n(\eta_s)$  and  $v_n(\eta)$ . This is an intrinsic feature in (3+1)D hydrodynamics with longitudinal fluctuations. One will indeed observe this feature in the comparison between longitudinal decorrelation of initial state  $\epsilon_3$  and final state  $v_3$ .

The decorrelation of initial eccentricities along spatial rapidity is defined analogously to Eq. (3) as,

$$r_n(\eta_s^a, \eta_s^b) = \frac{\langle \vec{\epsilon}_n(-\eta_s^a) \cdot \vec{\epsilon}_n^*(\eta_s^b) \rangle}{\langle \vec{\epsilon}_n(\eta_s^a) \vec{\epsilon}_n^*(\eta_s^b) \rangle}. \quad (7)$$

Shown in Fig. 6(a), the factorization ratio  $r_2(\eta_s^a, \eta_s^b)$  in coordinate space displays the same centrality dependence as the decorrelation of final-state hadrons shown in Fig. 7 for similar centralities of Pb+Pb collisions at  $\sqrt{s_{NN}} = 2.76$  TeV. For most central collisions, the decorrelation increases faster as  $\eta_s^a$  increases. For other centralities,  $r_2$  first increases from central to semi-peripheral and reaches a maximum at 20–30%, then it decreases for more peripheral collisions. The magnitude of the longitudinal decorrelation  $r_2$  in coordinate space is very close to decorrelation of final charged hadrons.

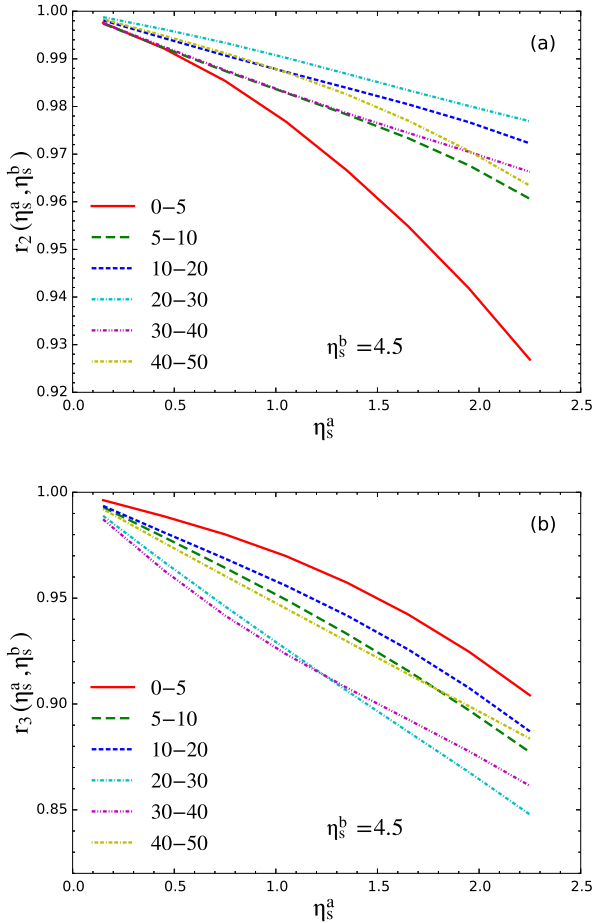


Figure 6: (Color online) (a) The factorization ratio  $r_2(\eta_s^a, \eta_s^b)$  and (b)  $r_3(\eta_s^a, \eta_s^b)$  for initial spatial eccentricity as a function of  $\eta_s^a$  for  $\eta_s^b = 4.5$  in Pb+Pb collisions at  $\sqrt{s_{NN}} = 2.76$  TeV from AMPT model in 6 different centralities.

The factorization ratio for the third-order initial eccentricity  $r_3(\eta_s^a, \eta_s^b)$  as shown in Fig. 6 (b), on the other

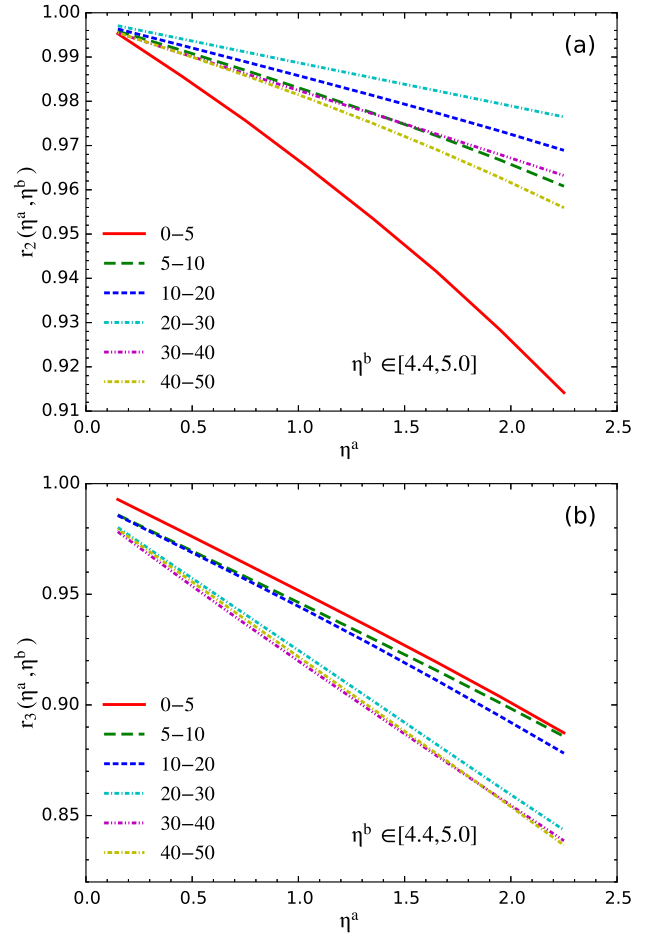


Figure 7: (Color online) (a) The factorization ratio  $r_2(\eta^a, \eta^b)$  and (b)  $r_3(\eta^a, \eta^b)$  for final charged hadrons from event-by-event hydrodynamics as a function of the pseudo rapidity  $\eta^a$  for  $\eta^b \in [4.4, 5.0]$  in Pb+Pb collisions at  $\sqrt{s_{NN}} = 2.76$  TeV for 6 centrality classes.

hand, decreases from the most central to peripheral collisions. The same centrality dependence is also observed in the factorization ratio of the anisotropic flow in the final state as shown in Fig. 7 (b). However, from mid-central to peripheral collisions there seems no particular order in the centrality dependence of the factorization ratio  $r_3$  for the initial eccentricity.

The definition of the factorization ratio is designed to remove short range correlations by correlating particles with large pseudo rapidity gaps. Therefore, the decorrelation of anisotropic flows along the longitudinal direction should not depend on the width of the Gaussian smearing in spatial rapidity in initial conditions from the AMPT model. Shown in Fig. 8 are factorization ratios for the initial eccentricity  $r_2(\eta_s^a, \eta_s^b)$  as a function of  $\eta_s^a$  in two centralities of Pb+Pb collisions at  $\sqrt{s_{NN}} = 2.76$  TeV with different values of the width  $\sigma_\eta = 0.4, 0.6, 0.8$  in the Gaussian smearing. Indeed, the factorization ratio shows no dependence on the smearing width.



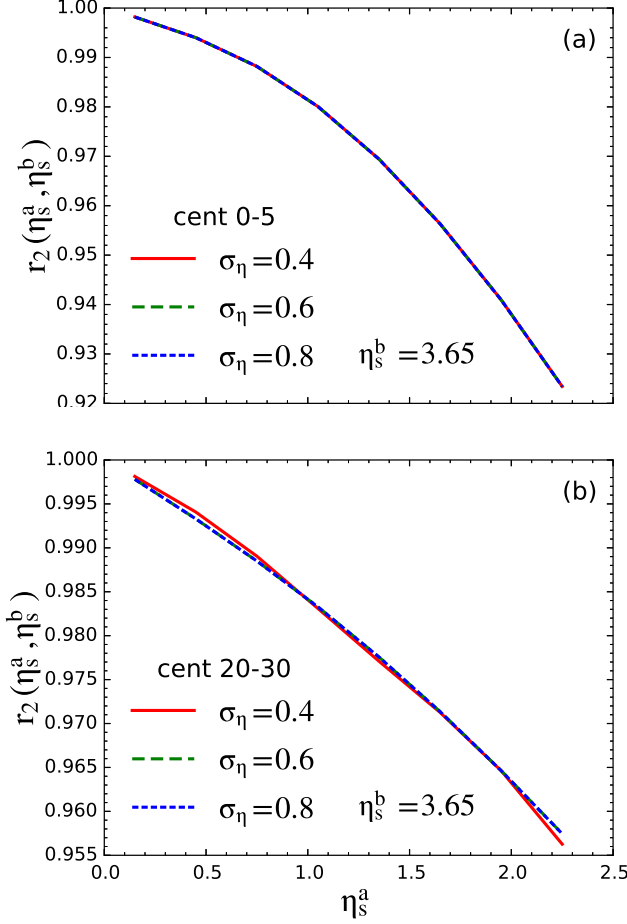


Figure 8: (Color online) The decorrelation function  $r_2(\eta_s^a, \eta_s^b)$  along spatial rapidity for different values of the width  $\sigma_{\eta_s}$  of the Gaussian smearing in the initial-state of Pb+Pb collisions at  $\sqrt{s_{NN}} = 2.76$  TeV from the AMPT model in the top (a) 0-5% and 20-30% centrality.

## V. TWIST OR RANDOM FLUCTUATIONS

There are two possible mechanisms for the decorrelation along the longitudinal direction. One is the twist of event plane angles and the other are random fluctuations along pseudo rapidity. In event-by-event (3+1)D hydrodynamics, without fluctuations due to finite number of particles in the final state, we can calculate event plane angles at different pseudo-rapidities  $\Psi_n(\eta)$  for each event, and study the fluctuation or twist structure for  $\Psi_n(\eta)$ .

Shown in Fig. 9 are event plane angles for 6 events in the top 0-5% centrality class from our (3+1)D hydrodynamic calculations as a function of  $\eta$  in Pb+Pb collisions at  $\sqrt{s_{NN}} = 2.76$  TeV. Some events have a clear twist structure, i.e., event plane angles  $\Psi_n$  monotonically increase or decrease along  $\eta$  direction. Some events do not have an apparent twist structure. Their event plane angles do not vary with  $\eta$  monotonically.

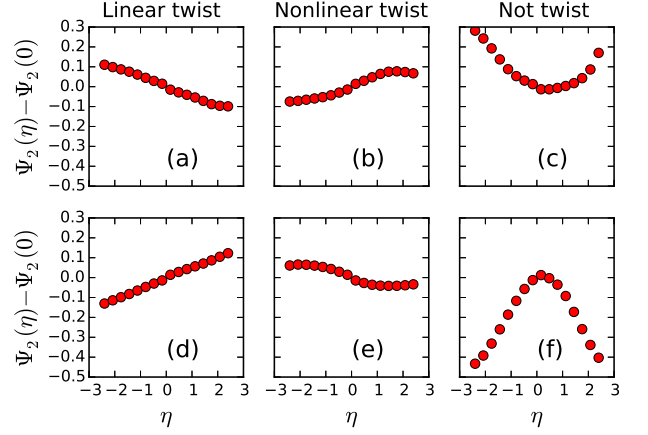


Figure 9: (Color online) The 2nd order event plane angles  $\Psi_2(\eta)$  as a function of pseudo-rapidity  $\eta$  for 6 typically selected events from event-by-event hydrodynamic simulations for 0-5% Pb+Pb collisions at  $\sqrt{s_{NN}} = 2.76$  TeV.

Typically there are events with a linear twist, nonlinear twist and events without twist as illustrated in Fig. 9. Probabilities for these 3 different types of events are studied by fitting the event plane angle  $\Psi_n(\eta)$  with a polynomial function  $\Psi_n(\eta) = a + b\eta + c\eta^2 + d\eta^3$ , where non-zero  $b$  denotes a linear twist of event plane angles. Non-zero polynomial coefficients  $c$  and  $d$  denote non-linear twist or pure fluctuations of event plane angles. Since the event averaged values of  $b$ ,  $c$  and  $d$  are equal to 0, we can use the standard deviations  $\sigma(x) = \langle (x - \langle x \rangle)^2 \rangle$  of these polynomial coefficients as a measure of fluctuation and decorrelation, as shown in Fig. 10 for 6 centrality classes of Pb+Pb collisions at  $\sqrt{s_{NN}} = 2.76$  TeV.

For the most central 0-5% collisions, the standard deviations of  $a$ ,  $b$ ,  $c$  and  $d$  in the 2nd order event plane angles are much bigger than in semi-central collisions. Large values of  $\sigma(a)$  indicate strong event-by-event fluctuations of the mean values of the event plane angle. One can see from Fig. 10 (a) that the 2nd order event plane angles fluctuate more in central collisions than in semi-central and peripheral collisions. A large value of  $\sigma(b)$  indicates that a strong decorrelation along the longitudinal direction comes from a linear twist of the event plane angles. The twist of the 2nd order event plane angles also have a strong centrality dependence as seen in Fig. 10 (a). On the other hand, standard deviations for coefficients of a polynomial fit to the 3rd event plane angles do not have any significant centrality dependence as shown in Fig. 10 (b).

Finite values of  $\sigma(c)$  and  $\sigma(d)$  indicates finite probabilities for the non-linear twist and pure fluctuations of event plane angles which are also bigger in the most central collisions. Over all, small standard deviations for  $c$  and  $d$  from both  $\Psi_2(\eta)$  in semi-central collisions and  $\Psi_3(\eta)$  in all centralities explain the linear behavior of the longitudinal decorrelation in these centralities.

Although hydrodynamic results underestimated  $r_2$



given by CMS experimental data in most central collisions, it has a similar feature as in CMS measurements that the decorrelation  $r_2$  is strongest in most central collisions. The discrepancy between the (3+1)D ideal hydrodynamic results and the CMS experimental data on decorrelation of the second order anisotropic flow in the most central collisions might be reduced by the introduction of viscosity in the hydrodynamic calculation. Since the shear viscosity reduces the expansion rate along  $\eta_s$  direction, it is possible that the decorrelation structure along the longitudinal direction for central collisions will also change.

The centrality dependence of the twist effect on the other hand agrees with predictions from the Glauber model [39], where the twist is strongest in most central collisions.

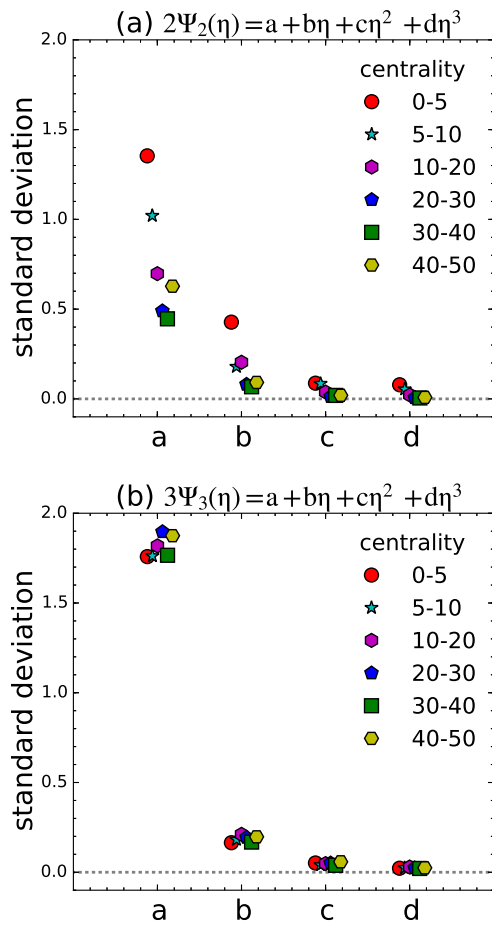


Figure 10: (Color Online) Standard deviation of fitting polynomial coefficients for  $\Psi_2(\eta)$  and  $\Psi_3(\eta)$ .

## VI. SUMMARY AND DISCUSSIONS

The decorrelation of 2nd and 3rd order anisotropic flow along the pseudo rapidity direction is investigated in

event-by-event (3+1)D ideal hydrodynamics with fluctuating initial conditions from the AMPT model for Pb+Pb collisions at LHC and Au+Au collisions at RHIC. With transverse and longitudinal fluctuations in AMPT model originating from pQCD+MC Glauber and string model, our results agree with CMS measurements for most of the available centralities. This suggests that the string model in HIJING model captures most of features of the longitudinal fluctuations along pseudo rapidity. Predictions for Au+Au collisions at RHIC show stronger longitudinal decorrelations, indicating larger fluctuations at lower energies. Further detailed study show that the longitudinal decorrelation in momentum space comes from initial state decorrelation in space.

In order to explain the non-linear behavior of  $r_2(\eta^a, \eta^b)$  in the most central collisions, event plane angles  $\Psi_n(\eta)$  for particles at different pseudo rapidities are calculated from event-by-event hydrodynamics for several characteristic events in the most central collisions. Some of these events show non-linear twist and pure fluctuations of event plane angles which provide the explanation for the non-linear behavior of  $r_2$  in most central collisions. By fitting  $\Psi_n(\eta)$  with a polynomial function, contributions from linear twist, non-linear twist and pure fluctuations are quantified by the standard deviations of polynomial coefficients. Larger standard deviations of non-linear polynomial coefficients in most central collisions make it clear that the non-linear twist and pure fluctuations are much bigger for  $r_2$  in 0 – 5% collisions. While very small non-linear polynomial coefficients in all centralities for  $\Psi_3(\eta)$  proves that the decorrelation of the 3rd order anisotropic flow comes mainly from linear twist of event plane angles.

The decorrelation of event plane angles and anisotropic flows along the longitudinal direction discussed in this paper have many consequences in the study of collective phenomena in high-energy collisions.

### $v_n$ measurements

Determination of event planes is crucial for  $v_n$  calculations. Most of current analysis methods use particles at forward or backward rapidity to determine event planes and calculate anisotropic flows for particles at mid rapidity. This method eliminates contributions to the anisotropic flows from short range correlations due to non-flow effects such as jets or fluid expansion of hot spots. These methods, however, assume rapidity-independent event planes and become problematic when event planes in different rapidity windows randomly fluctuate or are twisted.

The difference between event planes at  $\eta_a$  and  $-\eta_a$  has been attributed to the effect of finite multiplicities. This was assumed to be corrected by dividing the anisotropic flow  $\langle \cos(n(\phi - \Psi_n^A)) \rangle$  by a resolution factor

$$R = \sqrt{\frac{\langle \cos(n(\Psi_n^A - \Psi_n^B)) \rangle \langle \cos(n(\Psi_n^A - \Psi_n^C)) \rangle}{\langle \cos(n(\Psi_n^B - \Psi_n^C)) \rangle}}, \quad (8)$$

where  $\Psi_n^A$  and  $\Psi_n^B$  are event plane angles determined from particles at forward and backward rapidity windows and  $\Psi_C$  is the event plane angle at mid rapidity [39]. If event plane angles are linearly twisted along the pseudo rapidity direction, the decorrelation between  $\Psi_n^A$  and  $\Psi_n^C$  equals to the decorrelation between  $\Psi_n^B$  and  $\Psi_n^C$ , the resolution would become

$$R = R_0 \sqrt{\langle \cos(n(\Psi_n^+ - \Psi_n^-)) \rangle} \\ \approx R_0 \langle \cos(n(\Psi_n^+ - \Psi_n^0)) \rangle, \quad (9)$$

where  $R_0$  comes from the effect of a finite multiplicity while  $\langle \cos(n(\Psi_n^+ - \Psi_n^0)) \rangle$  stands for the decorrelation of the true event plane  $\Psi_n^+$  at forward rapidity and  $\Psi_n^0$  at mid rapidity. Approximately, currently used resolution factors give  $v_n = \langle \cos(n(\phi - \Psi_n^0)) \rangle$ , if the structure of longitudinal fluctuations is a global twist [48]. In this sense the event plane method is better than 2-particle correlation method in which a large pseudo rapidity gap is used to remove non-flow effects. The method using multiple particle cumulants without requiring a large pseudo rapidity gap is better for flow measurements.

If event planes in the final state are linearly twisted, which can be parameterized as  $\Psi_n(\eta) = b\eta$ , and the magnitude of  $v_n$  is the same for each rapidity slice in a rapidity window  $[-1, 1]$ , using the mean value of the event plane angle  $\Psi_n(\eta) = 0$  for all particles in this rapidity window will reduce  $v_n$  to  $v_n \sin(nb)/(nb)$ . The factor  $\sin(nb)/(nb)$  depends on the slope of the twist in  $\Psi_n(\eta)$  and the order of harmonic flows.

#### *Effects of longitudinal expansion.*

In a previous study [20], by changing the width of the rapidity window for determining event planes in (3+1)D hydrodynamics calculations, only a 6% difference has been observed coming from the decorrelation of event planes, the other 10 – 15% suppression of the elliptic flow originates from the coupling between transverse and longitudinal expansion. The additional gradient in the longitudinal direction between two adjacent spatial rapidity windows which have different spatial eccentricities and orientation angles can lead to an overall reduction in eccentricity and anisotropy flows of final particles. Notice that the measured decorrelation

of anisotropic flows along  $\eta$  is in momentum space. How such decorrelation is influenced by hydrodynamic expansion in longitudinal direction with fluctuating initial conditions and the effect of viscosity are interesting topics for further exploration.

#### *Long range di-hadron correlation in $\Delta\phi$*

Another observable that will be affected by the decorrelation of anisotropic flows is the di-hadron correlation as a function of azimuthal angle difference  $\Delta\phi$  and pseudo rapidity difference  $\Delta\eta$ . With a linear twist in event plane angles  $\Psi_n(\eta)$ , the di-hadron correlation function  $C_{12}(\Delta\eta, \Delta\phi)$  will have an intrinsic structure for the near-side and away-side ridge. In each single event, the ridge will be shifted from  $\Delta\phi = 0$  to  $\Delta\phi = 2b\Delta\eta$  on the near side and from  $\Delta\phi = \pi$  to  $\Delta\phi = \pi + 2b\Delta\eta$  on the away side, where  $b$  is the slope in the linear twist in  $\Psi_n(\eta) = b\eta$ . Since the slope  $b$  can be positive or negative, the event averaged di-hadron correlation will be broadened along  $\Delta\phi$  with a big pseudo rapidity gap [39].

#### **Acknowledgments**

We thank J. Jia, W. Li, P. Bozek, P. Huovinen and M. Gyulassy for helpful discussions. LGP and HP acknowledge funding of a Helmholtz Young Investigator Group VH-NG-822 from the Helmholtz Association and GSI. This work was supported in part by the Helmholtz International Center for the Facility for Antiproton and Ion Research (HIC for FAIR) within the framework of the Landes-Offensive zur Entwicklung Wissenschaftlich-Oekonomischer Exzellenz (LOEWE) program launched by the State of Hesse, by the Natural Science Foundation of China under Grants No. 11221504 and No. 11375072, by the Chinese Ministry of Science and Technology under Grant No. 2014DFG02050, and by the Director, Office of Energy Research, Office of High Energy and Nuclear Physics, Division of Nuclear Physics, of the U.S. Department of Energy under Contract No. DE-AC02-05CH11231. V.R. is supported by the Alexander von Humboldt foundation, Germany. Computational resources have been provided by the Center for Scientific Computing (CSC) at the Goethe-University of Frankfurt.

- 
- [1] Paul Romatschke and Ulrike Romatschke. Viscosity Information from Relativistic Nuclear Collisions: How Perfect is the Fluid Observed at RHIC? *Phys. Rev. Lett.*, 99:172301, 2007.
  - [2] Matthew Luzum and Paul Romatschke. Conformal Relativistic Viscous Hydrodynamics: Applications to RHIC results at  $\sqrt{s(NN)}^{1/2} = 200$ -GeV. *Phys. Rev.*, C78:034915, 2008. [Erratum: *Phys. Rev.* C79,039903(2009)].
  - [3] Huichao Song and Ulrich W. Heinz. Suppression of elliptic

- tic flow in a minimally viscous quark-gluon plasma. *Phys. Lett.*, B658:279–283, 2008.
- [4] Huichao Song and Ulrich W. Heinz. Causal viscous hydrodynamics in 2+1 dimensions for relativistic heavy-ion collisions. *Phys. Rev.*, C77:064901, 2008.
- [5] K. Dusling and D. Teaney. Simulating elliptic flow with viscous hydrodynamics. *Phys. Rev.*, C77:034905, 2008.
- [6] Denes Molnar and Pasi Huovinen. Dissipative effects from transport and viscous hydrodynamics. *J. Phys.*, G35:104125, 2008.

- [7] Piotr Bozek. Bulk and shear viscosities of matter created in relativistic heavy-ion collisions. *Phys. Rev.*, C81:034909, 2010.
- [8] A. K. Chaudhuri. Centrality dependence of elliptic flow and QGP viscosity. *J. Phys.*, G37:075011, 2010.
- [9] Bjorn Schenke, Sangyong Jeon, and Charles Gale. Elliptic and triangular flow in event-by-event (3+1)D viscous hydrodynamics. *Phys. Rev. Lett.*, 106:042301, 2011.
- [10] Bjorn Schenke, Sangyong Jeon, and Charles Gale. Higher flow harmonics from (3+1)D event-by-event viscous hydrodynamics. *Phys. Rev.*, C85:024901, 2012.
- [11] Tetsufumi Hirano and Yasushi Nara. Eccentricity fluctuation effects on elliptic flow in relativistic heavy ion collisions. *Phys. Rev.*, C79:064904, 2009.
- [12] B. Alver and G. Roland. Collision geometry fluctuations and triangular flow in heavy-ion collisions. *Phys. Rev.*, C81:054905, 2010. [Erratum: *Phys. Rev.* C82:039903(2010)].
- [13] Burak Han Alver, Clement Gombeaud, Matthew Luzum, and Jean-Yves Ollitrault. Triangular flow in hydrodynamics and transport theory. *Phys. Rev.*, C82:034913, 2010.
- [14] A. Adare et al. Measurements of Higher-Order Flow Harmonics in Au+Au Collisions at  $\sqrt{s_{NN}} = 200$  GeV. *Phys. Rev. Lett.*, 107:252301, 2011.
- [15] Ekaterina Retinskaya, Matthew Luzum, and Jean-Yves Ollitrault. Constraining models of initial conditions with elliptic and triangular flow data. *Phys. Rev.*, C89(1):014902, 2014.
- [16] Chun Shen, Zhi Qiu, and Ulrich Heinz. Shape and flow fluctuations in ultracentral Pb + Pb collisions at the energies available at the CERN Large Hadron Collider. *Phys. Rev.*, C92(1):014901, 2015.
- [17] Wojciech Broniowski, Piotr Bozek, and Maciej Rybczynski. Fluctuating initial conditions in heavy-ion collisions from the Glauber approach. *Phys. Rev.*, C76:054905, 2007.
- [18] Hannah Petersen, Jan Steinheimer, Gerhard Burau, Marcus Bleicher, and Horst Stocker. A Fully Integrated Transport Approach to Heavy Ion Reactions with an Intermediate Hydrodynamic Stage. *Phys. Rev.*, C78:044901, 2008.
- [19] K. Werner, Iu. Karpenko, T. Pierog, M. Bleicher, and K. Mikhailov. Event-by-Event Simulation of the Three-Dimensional Hydrodynamic Evolution from Flux Tube Initial Conditions in Ultrarelativistic Heavy Ion Collisions. *Phys. Rev.*, C82:044904, 2010.
- [20] Longgang Pang, Qun Wang, and Xin-Nian Wang. Effects of initial flow velocity fluctuation in event-by-event (3+1)D hydrodynamics. *Phys. Rev.*, C86:024911, 2012.
- [21] Charles Gale, Sangyong Jeon, and Bj Schenke.
- [22] Guo-Liang Ma and Xin-Nian Wang. Jets, Mach cone, hot spots, ridges, harmonic flow, dihadron and  $\gamma$ -hadron correlation in high-energy heavy-ion collisions. *Phys. Rev. Lett.*, 106:162301, 2011.
- [23] K. Aamodt et al. Harmonic decomposition of two-particle angular correlations in Pb-Pb collisions at  $\sqrt{s_{NN}} = 2.76$  TeV. *Phys. Lett.*, B708:249–264, 2012.
- [24] Ulrich Heinz, Zhi Qiu, and Chun Shen. Fluctuating flow angles and anisotropic flow measurements. *Phys. Rev.*, C87(3):034913, 2013.
- [25] Fernando G. Gardim, Frederique Grassi, Matthew Luzum, and Jean-Yves Ollitrault. Breaking of factorization of two-particle correlations in hydrodynamics. *Phys. Rev.*, C87(3):031901, 2013.
- [26] Zhi Qiu and Ulrich Heinz. Hydrodynamic event-plane correlations in Pb+Pb collisions at  $\sqrt{s} = 2.76$  ATeV. *Phys. Lett.*, B717:261–265, 2012.
- [27] Zhi Qiu. *Event-by-event Hydrodynamic Simulations for Relativistic Heavy-ion Collisions*. PhD thesis, Ohio State U., 2013.
- [28] Hannah Petersen, Vivek Bhattacharya, Steffen A. Bass, and Carsten Greiner. Longitudinal correlation of the triangular flow event plane in a hybrid approach with hadron and parton cascade initial conditions. *Phys. Rev.*, C84:054908, 2011.
- [29] Kai Xiao, Feng Liu, and Fuqiang Wang. Event-plane decorrelation over pseudorapidity and its effect on azimuthal anisotropy measurements in relativistic heavy-ion collisions. *Phys. Rev.*, C87(1):011901, 2013.
- [30] Long-Gang Pang, Guang-You Qin, Victor Roy, Xin-Nian Wang, and Guo-Liang Ma. Longitudinal decorrelation of anisotropic flows in heavy-ion collisions at the CERN Large Hadron Collider. *Phys. Rev.*, C91(4):044904, 2015.
- [31] A. Adil, M. Gyulassy, and T. Hirano. 3D jet tomography of the twisted color glass condensate. *Phys. Rev.*, D73:074006, 2006.
- [32] A. Adil and M. Gyulassy. 3D jet tomography of twisted strongly coupled quark gluon plasmas. *Phys. Rev.*, C72:034907, 2005.
- [33] Piotr Bozek, Wojciech Broniowski, and Joao Moreira. Torqued fireballs in relativistic heavy-ion collisions. *Phys. Rev.*, C83:034911, 2011.
- [34] N. Borghini, P. M. Dinh, and J. Y. Ollitrault. Analysis of directed flow from three particle correlations. *Nucl. Phys.*, A715:629–632, 2003.
- [35] The ATLAS collaboration. Measurement of two-particle pseudorapidity correlations in lead-lead collisions at  $\sqrt{s_{NN}} = 2.76$  TeV with the ATLAS detector. 2015.
- [36] Akihiko Monnai and Bjoern Schenke. Pseudorapidity correlations in heavy ion collisions from viscous fluid dynamics. 2015.
- [37] Piotr Bozek, Wojciech Broniowski, and Adam Olszewski. Two-particle correlations in pseudorapidity in a hydrodynamic model. 2015.
- [38] Peng Huo, Jiangyong Jia, and Soumya Mohapatra. Elucidating the event-by-event flow fluctuations in heavy-ion collisions via the event shape selection technique. *Phys. Rev.*, C90(2):024910, 2014.
- [39] Jiangyong Jia and Peng Huo. Forward-backward eccentricity and participant-plane angle fluctuations and their influences on longitudinal dynamics of collective flow. *Phys. Rev. C*, 90:034915, Sep 2014.
- [40] Vardan Khachatryan et al. Evidence for transverse momentum and pseudorapidity dependent event plane fluctuations in PbPb and pPb collisions. 2015.
- [41] Long-Gang Pang, Yoshitaka Hatta, Xin-Nian Wang, and Bo-Wen Xiao. Analytical and numerical Gubser solutions of the second-order hydrodynamics. *Phys. Rev.*, D91(7):074027, 2015.
- [42] Zi-Wei Lin, Che Ming Ko, Bao-An Li, Bin Zhang, and Subrata Pal. A Multi-phase transport model for relativistic heavy ion collisions. *Phys. Rev.*, C72:064901, 2005.
- [43] Pasi Huovinen and Pter Petreczky. QCD Equation of State and Hadron Resonance Gas. *Nucl. Phys.*, A837:26–53, 2010.
- [44] Xin-Nian Wang and Miklos Gyulassy. HIJING: A Monte Carlo model for multiple jet production in p p, p A and

- A A collisions. *Phys. Rev.*, D44:3501–3516, 1991.
- [45] Piotr Bozek and Wojciech Broniowski. The torque effect and fluctuations of entropy deposition in rapidity in ultra-relativistic nuclear collisions. 2015.
  - [46] Ehab Abbas et al. Centrality dependence of the pseudorapidity density distribution for charged particles in Pb-Pb collisions at  $\sqrt{s_{NN}} = 2.76$  TeV. *Phys.Lett.*, B726:610–622, 2013.
  - [47] Georges Aad et al. Measurement of the pseudorapidity and transverse momentum dependence of the elliptic flow of charged particles in lead-lead collisions at  $\sqrt{s_{NN}} = 2.76$  TeV with the ATLAS detector. *Phys. Lett.*, B707:330–348, 2012.
  - [48] Wei Li. Longitudinal decorrelations of flow orientation angle in AA and pA. *INT work shop, 2015 Seattle*.